DYNA
http://dyna.medellin.unal.edu.co/

UNIVERSIDAD NACIONAL DE COLOMBIA

Design and evaluation of a high-speed centrifugal precision seed-metering device for soybean based on DEM simulation

Yujie Zhang, Xianliang Wang, Xiupei Cheng, Zhongcai Wei, Pingchuan Ma & Xiangcai Zhang*

*Institute of Modern Agricultural Equipment, Shandong University of Technology, Xincun West Rd, Zibo255049, China. zyjhk1989@163.com, wxl1990@sdut.edu.cn, cheng2021@sdut.edu.cn, weizc@sdut.edu.cn, ashley494@163.com, *Corresponding author: zxcai0216@163.com*

Received: July 16th, 2025. Received in revised form: December 15th, 2025. Accepted: December 29th, 2025.

Abstract
A high-speed centrifugal precision seed metering device for soybeans was developed to improve single-seed sowing accuracy under high-speed operation. The device integrates an involute deflector strip and ellipsoidal seed grooves, driven by a stepper motor to control the centrifugal disc and seed-metering wheel. Using EDEM software, a simulation model was established. A quadratic orthogonal design was applied with deflector type, disc speed, and seed-metering wheel speed as factors, and qualified seeding rate and miss rate as indicators. The optimal combination—disc speed of 49.01 r/min and wheel speed of 593.75 r/min—achieved a 92.08% seeding qualification rate and 1.91% miss rate. Bench tests confirmed strong agreement with simulation results, verifying the system's reliability. This study offers a theoretical and practical reference for the development of high-speed precision metering devices for soybean planting.

Keywords: **p**recision soybean sowing; centrifugal type; high-speed metering; DEM.

Diseño y evaluación de un dispositivo de dosificación de semillas de precisión centrífuga de alta velocidad para soja basado en simulación DEM

Resumen
Se diseñó un dispositivo dosificador centrífugo de alta velocidad para la siembra de precisión de soya, con el fin de mejorar la eficiencia y la calidad en la dosificación unitaria de semillas bajo condiciones de alta velocidad. El sistema incorpora tiras deflectoras de perfil involuto y cavidades de almacenamiento elipsoidales, accionadas por un motor paso a paso que regula el disco centrífugo y el rotor dosificador. Se desarrolló un modelo de simulación mediante el software EDEM, y se aplicó un diseño experimental ortogonal rotacional con tres factores: tipo de deflector, velocidad del disco y velocidad del rotor. Los resultados óptimos (49.01 r/min y 593.75 r/min) alcanzaron una tasa de dosificación correcta del 92.08 % y una tasa de fallos del 1.91 %. Las pruebas en banco confirmaron la fiabilidad del dispositivo. Este estudio proporciona una base técnica y experimental para el desarrollo de dosificadores de precisión centrífugos en la mecanización agrícola.

Palabras clave: siembra de precisión de soya; dosificador centrífugo; alta velocidad; DEM.

1 Introduction

As the core component of a precision planter [1], the seed-metering device significantly influences the efficiency and quality of sowing operations [2,3]. At present, precision seed-metering devices in use worldwide can be generally categorized into two types: mechanical and pneumatic [4-6]. Mechanical seed-metering devices are widely adopted in soybean, maize, and other crop planting due to their compact structure, low manufacturing cost, and strong adaptability.

However, conventional mechanical seed metering devices often suffer from low filling efficiency, unstable discharge, and seed damage at high speeds, limiting their suitability for modern precision sowing [8]. Liu et al. [9] found that high-speed operation significantly reduces filling stability, leading to seed overlap, bounce, or breakage. Teixeira et al. [10] noted that poor structural design increases seed friction and damage, resulting in missed or repeated seeding. Most centrifugal metering

How to cite: Zhang, Y., Wang, X., Cheng, X., Wei, Z., Ma, P., and Zhang, X., Design and evaluation of a high-speed centrifugal precision seed-metering device for soybean based on DEM simulation DYNA, (93)240, pp. 53-61, January - March, 2026.

systems are still limited to row sowing, with limited application in single-seed precision sowing for crops like soybean [11].

To address these issues, this study proposes a novel high-speed centrifugal precision metering device for soybean. The device employs structural innovations and optimized seed flow guidance to improve uniformity and reliability. Furthermore, DEM-based simulations are used to analyze seed kinematics, and a response surface methodology (RSM) is applied to optimize key structural parameters. Finally, bench tests are conducted to validate the simulation results. The study aims to provide both theoretical insights and practical support for engineering applications of centrifugal seed metering systems.

2 Structure and working principle of the seed metering device

2.1 Structural design

The developed high-speed centrifugal precision soybean seed metering device primarily consists of the housing, seed scraper, slender shaft, seed-metering wheel, centrifugal disc, seed discharge unit, and main shaft. A schematic of the overall structure is shown in Fig. 1.

The centrifugal unit comprises a main shaft, centrifugal disc, guide strips, and ellipsoidal seed-holding cavities. The disc is directly driven by a stepper motor through the main shaft, generating centrifugal force during high-speed rotation. This force, in combination with the deflector strips, induces seed dispersion and directional flow. To improve seeding accuracy, ellipsoidal cavities are adopted instead of traditional metering holes, with dimensions optimized according to soybean seed geometry.

The seed-metering unit consists of a flexible seed-metering wheel mounted on the slender shaft, made of elastic composite material with favorable wear resistance and buffering capacity, effectively minimizing seed damage. The device includes two symmetric seed outlets, each equipped with a scraper that removes overlapped

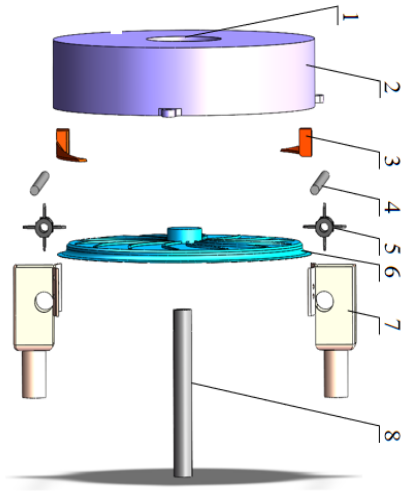

Figure 1. Structural diagram of the high-speed centrifugal precision seed metering device. 1. Seed inlet 2. Housing 3. Seed scraper 4. Slender shaft 5. Seed-metering wheel 6. Centrifugal disc 7. Seed discharge unit 8. Main shaft.
Source: Elaborated by the authors.

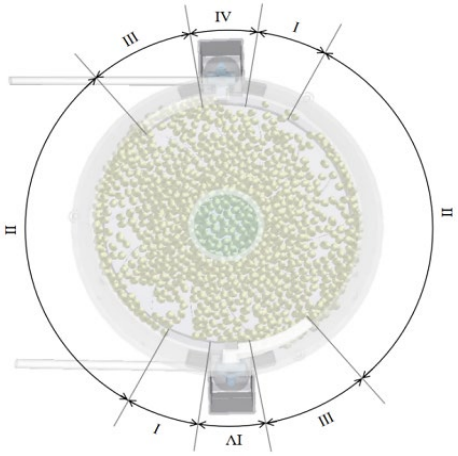

Figure 2. Structural diagram of the working principle of the seed metering device
Source: Elaborated by the authors.

or misaligned seeds, ensuring accurate single-seed discharge. The configuration allows dual-row operation with a single device, improving field productivity.

2.2 Working principle

Prior to operation, seeds enter the device through the inlet and fall onto the centrifugal disc under gravity. The seed metering process consists of four stages (Fig. 2):

- Centrifugation: The high-speed rotation of the disc generates centrifugal force, dispersing seeds toward the perimeter and partially into the cavities.
- Seed Filling: Under the combined action of centrifugal force and inter-particle interactions, seeds are evenly distributed and pressed against the inner wall of the housing, completing cavity filling.
- Seed Scraping: As the disc rotates further, seeds reach the scraper region, where overlapped or misoriented seeds are removed to ensure accurate single-seed positioning.
- Seed Discharge: At the discharge outlet, seeds are pushed into the outlet passage by the seed-metering wheel, aided by centrifugal force, achieving single-seed delivery.

Through the coordinated design of internal structures and dynamic intervention, the device ensures stable and precise seed discharge even at high operational speeds, supporting high-efficiency precision planting.

3 Design of key structural parameters

3.1 Geometric characteristics of soybean seeds

To ensure accurate structural matching and optimal design, it is essential to quantify the physical properties of the target seeds. In this study, the soybean cultivar "Shangdou 1201" was selected as the target material. Using a CHNT digital caliper (range: 0–150 mm; resolution: 0.01 mm), 1000 seeds were randomly sampled, and their principal dimensions were measured in accordance with the method illustrated in Fig. 3 [12].

Through calculation [13], the average seed length (L) of 8.74 mm, width (W) of 7.61 mm, and thickness (T) of 6.47 mm. The geometric mean diameter (Dg) was calculated as 7.55 mm, with a sphericity of 86.29% and a coefficient of variation of 12.32%, indicating moderate dimensional variability.

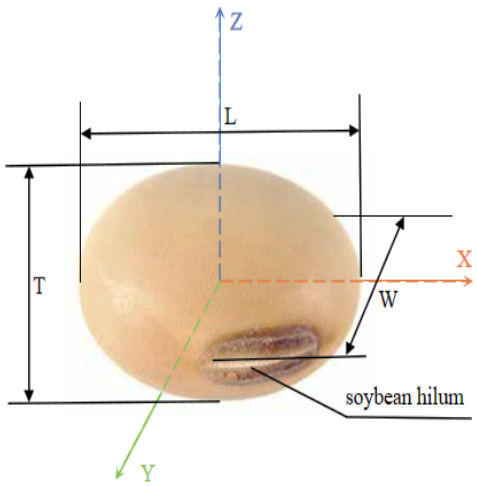

Figure 3. Schematic diagram of soybean tri-axial dimensions.
Source: Elaborated by the authors.

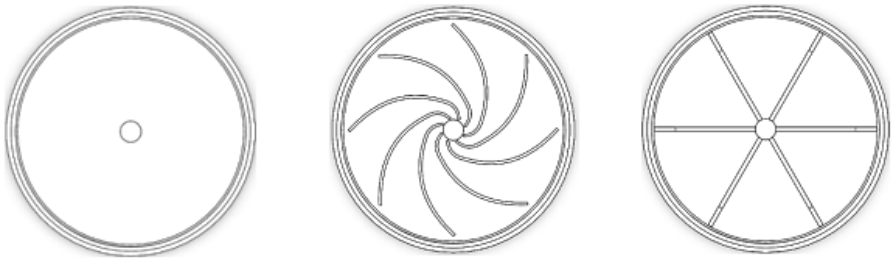

Figure 4. Comparison of deflector bar types. a. No deflector strip b. Involute profile c. Rectangular.
Source: Elaborated by the authors.

3.2 Centrifugal disc design

3.2.1 Guide strip configuration

As a critical structural element, the guide strip determines the disturbance and trajectory control of seeds during centrifugal motion. Three guide configurations were considered in this study: no guide strip, involute guide strip, and rectangular guide strip (Fig. 4).

During seed dispersion, forces acting on a seed include centrifugal force (Fa), gravity (G), inter-particle interaction (Fp), and support forces from the disc and guide surface (N1, N2). A simplified force analysis diagram is shown in Fig. 5, Fc represents the resultant force of the seed along the radial plane of the centrifugal disc, with the frictional force between the seed and the centrifugal disc ignored.

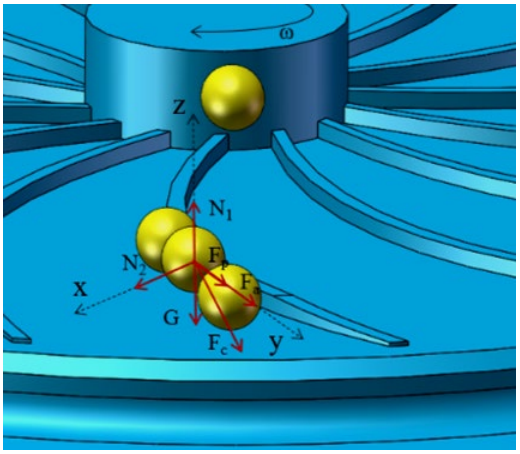

Figure 5. Force analysis of the seed-throwing process.
Source: Elaborated by the authors.

$$F_c = F_a + F_p + G + N_1 + N_2 \quad (1)$$

3.2.2 Groove geometry for seed holding

The seed-holding groove is the key structural unit responsible for retaining and discharging single seeds. Based on the geometric mean diameter of the soybean seeds, the groove diameter was set at 12.08mm [14,15].

Typical seed postures within the groove were classified as tangential, radial, and upright (Fig. 6). Among these, the tangential posture was the most stable and desirable. Inappropriate groove dimensions could result in partial insertion, dual occupancy, or seed escape (Fig.7). To verify the rationality of the seed-holding groove parameters, discrete element simulations were subsequently conducted to analyze the dynamic filling behavior and static stability distribution of seeds within the grooves. Ensure not only sufficient geometric capacity but also enhanced seed guidance and resistance to operational disturbance.

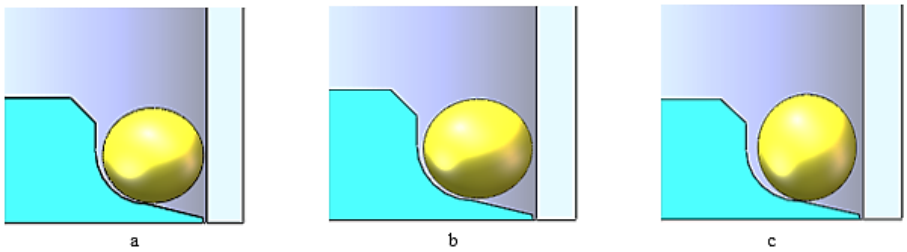

Figure 6. Illustration of typical seed postures during the filling process. a. Tangential state b. Radial state c. Upright state.
Source: Elaborated by the authors.

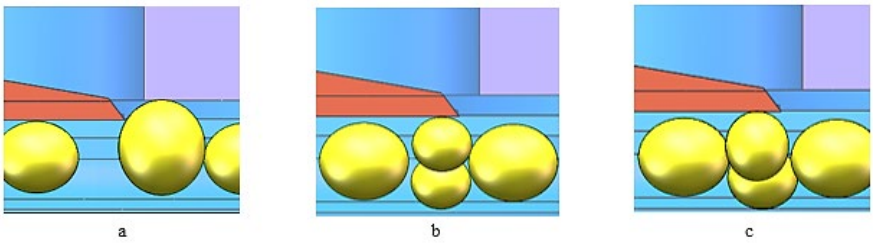

Figure 7. Analysis of missed-seeding and double-seeding scenarios. a. Miss seeding b. First repeated seeding c. Second repeated seeding.
Source: Elaborated by the authors.

3.3 Seed-metering wheel design

The seed-metering wheel operates at the final stage of the metering cycle, assisting in the extraction and directed discharge of seeds. Its structural parameters directly affect metering continuity and discharge quality.

A four-blade configuration was adopted and the blades were fabricated from high-strength rubber, chosen for its moderate elasticity and superior abrasion resistance. A concave arc was incorporated into the blade tips to enhance seed guidance while minimizing collision and scraping. This structure proved effective in adapting to seed variability and maintaining discharge consistency.

During operation, seeds were subjected to centrifugal force (F_c) from the disc and tangential pushing force (F_t) from the seed-metering wheel (Fig. 8). The introduction of this flexible metering mechanism significantly improved the adaptability of the system under high-speed conditions and contributed to stable single-seed output.

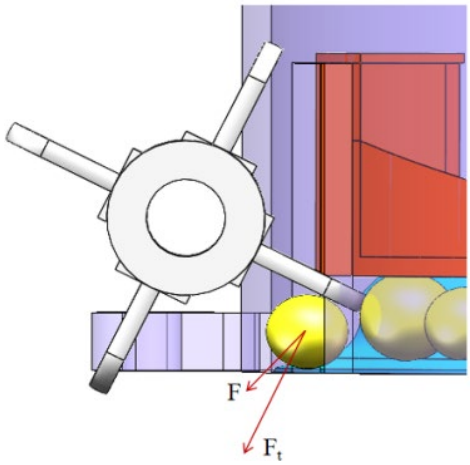

Figure 8. Force analysis diagram of the seed metering process.
Source: Elaborated by the authors.

4 Discrete element simulation

4.1 Global simulation parameters

The non-standard parts of this device were manufactured using 3D printing technology using Somos 8000 resin, while the blades of the seed-metering wheel were made of rubber material. In order to optimize the working effect of the seed drop stage, this paper uses the discrete element software EDEM to carry out simulation tests, and the contact model uses the Hertz-Mindlin no-slip [16] contact model, and the global variable parameters [17] are set as shown in Table 1.

Table 1.
DEM simulation parameter settings.

Material Pair	Parameter	Value
Soybean	Poisson's ratio	0.23
	Shear modulus (Pa)	6.3×10^{7}
	Density (kg·m^{-3})	1290
Resin	Poisson's ratio	0.35
	Shear modulus (Pa)	1.2×10^{8}
	Density (kg·m^{-3})	1454.7
Rubber	Poisson's ratio	0.40
	Shear modulus (Pa)	1.0×10^{6}
	Density (kg·m^{-3})	1250
Soybean–Soybean	Restitution coefficient	0.60
	Static friction coefficient	0.45
	Rolling friction coefficient	0.05
Soybean–Resin	Restitution coefficient	0.32
	Static friction coefficient	0.45
	Rolling friction coefficient	0.04
Soybean–Rubber	Restitution coefficient	0.50
	Static friction coefficient	0.60
	Rolling friction coefficient	0.10

Source: Elaborated by the authors.

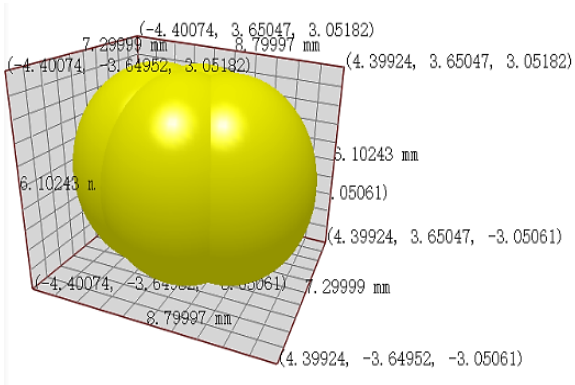

Figure. 9 Soybean particle model.
Source: Elaborated by the authors.

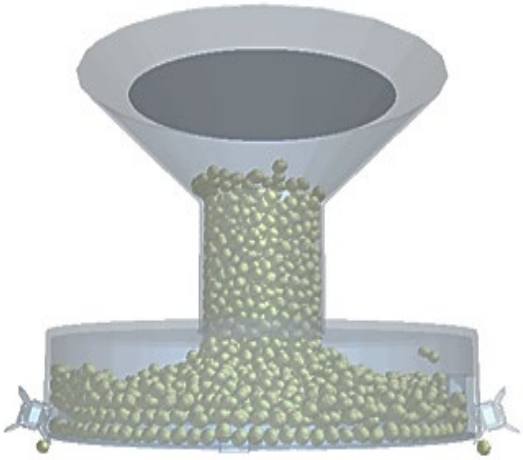

Figure. 10 Simplified model of the seed-metering device in EDEM.
Source: Elaborated by the authors.

4.2 Simulation model construction

To realistically capture seed dynamics during the metering process [18], a virtual simulation environment was constructed using EDEM 2020. Given that the soybean seeds exhibited a sphericity of 86.29%, they were approximated using a four-sphere cluster model (Fig. 9).

A simplified CAD model of the seed-metering device was developed in SolidWorks and exported in STL format. Only the critical contact components—centrifugal disc, housing, scraper, and seed-metering wheel—were retained in the EDEM environment to reduce computational complexity. Rotational motion parameters for the disc and the seed-metering wheel were defined using the Add-in Motion module to simulate realistic high-speed operating conditions. The simplified model is shown in Fig. 10.

4.2 Design of simulation experiments

To systematically investigate the influence of structural parameters on metering performance, a second-order orthogonal rotation combination design was employed. The guide strip type, centrifugal disc speed, and seed-metering wheel speed were selected as independent variables, while the seeding qualification index and miss-seeding index were taken as response variables. The factor level coding is shown in Table 2.

Table 2.
Factor levels in simulation.

Code	X_1 (Strip type)	X_2 (Disc speed, r/min)	X_3 (Wheel speed, r/min)
-1	No strip	45	550
0	Involute strip	50	600
1	Rectangular strip	55	650

Source: Elaborated by the authors.

4.3 Simulation procedure and observations

To capture the dynamic behavior of seeds within the internal mechanisms, visual tracking and particle state analysis were performed throughout a complete metering cycle. Snapshots from key simulation time steps are shown in Fig. 11.

At t = 0.15 s, seeds were uniformly released from the particle factory and fell under gravity into the rotating centrifugal disc. Due to high rotational speed, seeds immediately experienced substantial radial acceleration.

By t = 0.56 s, seeds were being guided outward by the disturbance of the guide strip and began accumulating near the groove regions. Minor collisions and friction-induced reorientation were observed.

At t = 0.61 s, some grooves contained double seeds due to particle variability or stacking angles. The scraper began to intervene, selectively removing misaligned or excess seeds while preserving properly oriented single seeds.

By t = 1.12-1.15 s, the seed-metering wheel engaged with the groove region. The flexible blades made gentle contact and applied tangential thrust. Under combined centrifugal and tangential forces, seeds were smoothly pushed out of the groove and guided into the discharge chute, completing the single-seed metering cycle.

Comprehensive statistical analysis across multiple simulation cycles revealed that filling efficiency, discharge stability, and miss-seeding rate were highly correlated with the rotational speeds of both the centrifugal disc and the seed-metering wheel, confirming a strong coupling between structural parameters and the dynamic behavior of
the seed-metering process. This analysis provided a solid theoretical foundation for subsequent parameter optimization and experimental validation.

4.5 Simulation results and statistical analysis

A total of 17 simulation trials were conducted based on the Box–Behnken response surface methodology [19], with each trial repeated three times under identical conditions. The average values of the qualified seeding index (Y_1) and the miss-seeding index (Y_2) were used for subsequent statistical analysis. The test results are presented in Table 3, while the analysis of variance (ANOVA) [20,21] for the regression models is summarized in Table 4.

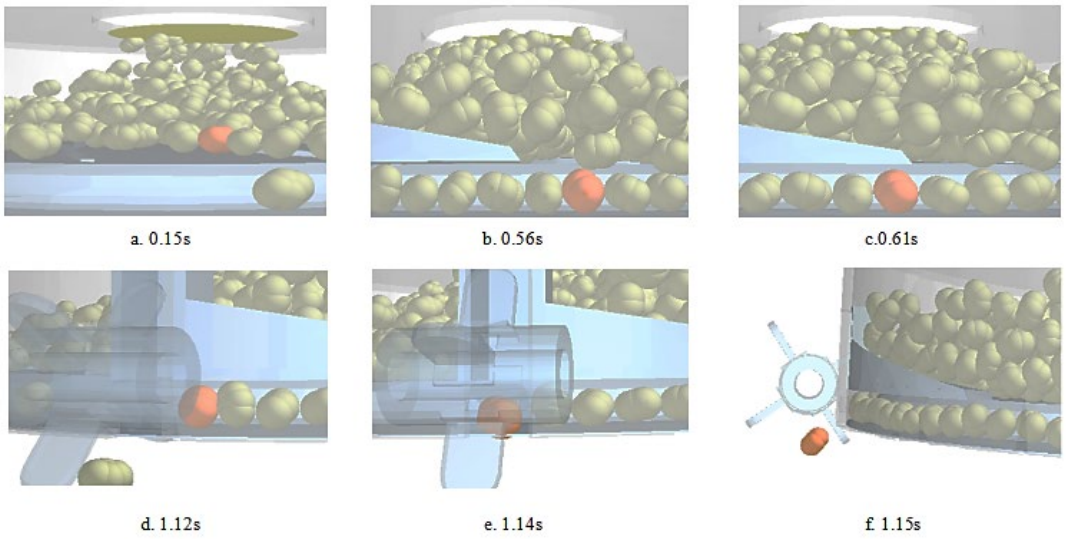

Figure 11. Snapshots of the simulated seeding process in EDEM.
Source: Elaborated by the authors.

Table 3.
Test protocol and results.

Test serial number	Test factor			Test index	
	X_1	X_2	X_3	Qualified index/Y_1(%)	Leakage index/Y_2(%)
1	-1	0	1	90.49	3.23
2	0	0	0	92.35	2.66
3	1	0	-1	88.68	2.86
4	0	1	1	88.43	3.94
5	1	1	0	86.44	2.22
6	0	0	0	92.03	2.03
7	0	-1	-1	88.92	3.25
8	-1	1	0	89.76	2.18
9	0	0	0	92.42	2.92
10	1	0	1	88.65	1.56
11	0	0	0	92.11	2.19
12	0	1	-1	88.24	2.73
13	-1	-1	0	87.73	2.42
14	0	0	0	91.94	4.31
15	-1	0	-1	88.96	3.29
16	0	-1	1	89.55	2.14
17	1	-1	0	90.12	3.63

Source: Elaborated by the authors.

Table 4.
Regression model variance analysis.

Variance source	Qualified seeding index				Miss-seeding index			
	Sum of squares	Degree of freedom	*F*	*P*	Sum of Squares	Degree of freedom	*F*	*P*
Model	52.43	9	99.79	< 0.0001	8.37	9	17.70	0.0005
A	1.16	1	19.92	0.0029	1.39	1	26.53	0.0013
B	1.49	1	25.49	0.0015	1.10	1	20.98	0.0025
C	0.6728	1	11.53	0.0115	1.03	1	19.59	0.0031
AB	8.15	1	139.63	< 0.0001	0.1892	1	3.60	0.0996
AC	0.6084	1	10.42	0.0145	0.1406	1	2.68	0.1459
BC	0.0484	1	0.8291	0.3928	0.1764	1	3.36	0.1096
A^2	11.1	1	190.17	< 0.0001	1.97	1	37.53	0.0005
B^2	17.42	1	298.34	< 0.0001	1.43	1	27.13	0.0012
C^2	7.69	1	131.7	< 0.0001	0.5217	1	9.93	0.0161
Residual error	0.4086	7			0.3679	7		
Misfit term	0.2376	3	1.85	0.2782	0.0630	3	0.2756	0.8410
Pure error	0.171	4			0.3049	4		
Sum	52.84	16			8.74	16		

Source: Elaborated by the author.

The results indicated that the regression models for both the qualified seeding index (Y_1) and the miss-seeding

index (Y_2) were highly significant (P<0.01), while the residuals and lack-of-fit terms were not statistically significant (P>0.05), confirming the overall adequacy and goodness-of-fit of the models.

For the Y_1 model, the main effects A (guide strip type), B (disc speed), and C (seed-metering wheel speed), as well as the interaction terms AB and AC, and the quadratic terms A^2, B^2, and C^2, were all highly significant (P<0.01). The interaction term BC was found to be statistically insignificant.

For the Y_2 model, the main effects A, B, and C, along with their respective quadratic terms A^2, B^2, and C^2, were all highly significant (P<0.01), while all interaction terms showed no significant influence.

After eliminating the coefficients of factors with insignificant effects from the regression equation, the quadratic regression equation between the evaluation index and the experimental factors is established as follows:

$$\begin{cases} Y_1 = 92.17 - 0.38X_1 - 0.43X_2 + 0.29X_3 - 1.43X_1X_2 \\ \quad -0.39X_1X_3 - 1.62X_1^2 - 2.03X_2^2 - 1.35X_3^2 \\ Y_2 = 2.04 - 0.42X_1 + 0.37X_2 + 0.36X_3 \\ \quad +0.68X_1^2 + 0.58X_2^2 + 0.35X_3^2 \end{cases} \quad (2)$$

To further visualize the relationships between test factors and response variables, response surface plots were generated for interactions with statistically significant effects. The results are illustrated in Fig. 12-13.

The response surface diagrams (Figs. 10-11) clearly revealed the variation trends of the parameters: the qualified seeding index (Y_1) increased initially and then declined with rising values of disc speed (X_2) and seed-metering wheel speed (X_3), with the optimal range identified at approximately 49–51 r/min for X_2 and 590–610 r/min for X_3. Superior metering performance was achieved when the guide strip profile of the centrifugal disc was of the involute type. In contrast, the miss-seeding index (Y_2) exhibited a typical "U-shaped" trend, decreasing first and then increasing with respect to X_2 and X_3, indicating the existence of an optimal operating region. The type of guide strip showed no significant effect on Y_2.

4.6 Parameter optimization

Based on the regression models obtained from the simulation experiments [22,23], a multi-objective optimization was performed with the goal of maximizing the qualified seeding index (Y_1) while minimizing the miss-seeding index (Y_2). The Design-Expert software was used to perform a global numerical optimization within the feasible design space.

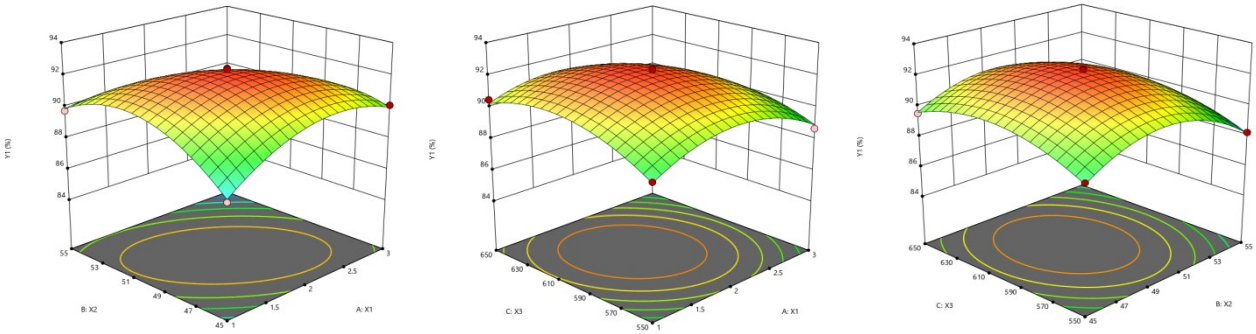

a. $Y_1=f(X_1,\ X_2,\ 600)$ b. $Y_1=f(X_1,\ 50,\ X_3)$ c. $Y_1=f(2,\ X_2,\ X_3)$

Figure 12. Effect of Factor Interactions on Qualified Seeding Index (Y_1).
Source: Elaborated by the authors.

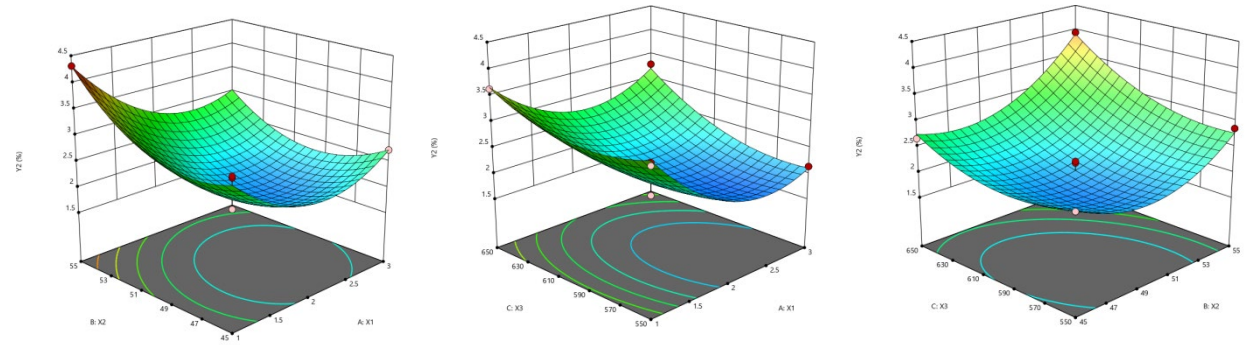

a. $Y_2=f(X_1,\ X_2,\ 600)$ b. $Y_2=f(X_1,\ 50,\ X_3)$ c. $Y_2=f(2,\ X_2,\ X_3)$

Figure 13. Effect of Factor Interactions on Miss-Seeding Index (Y_2).
Source: Elaborated by the authors.

$$\begin{cases} \max Y_1(X_1, X_2, X_3) \\ \min Y_2(X_1, X_2, X_3) \\ \text{s.t.} \begin{cases} 1 \le X_1 \le 3 \\ 45\text{r/min} \le X_2 \le 55\text{r/min} \\ 550\text{r/min} \le X_3 \le 650\text{r/min} \end{cases} \end{cases} \quad (3)$$

Under the constraints of structural feasibility and realistic operating conditions, the optimal combination of parameters was determined as follows:

- Guide strip type (X_1): involute profile
- Centrifugal disc speed (X_2): 49.01 r/min
- seed-metering wheel speed (X_3): 593.75 r/min

At these parameter values, the simulation predicted a qualified seeding index of 92.08% and a miss-seeding index of 1.91%, both of which satisfy the performance requirements for high-speed precision planting. These results provide a reliable reference point for experimental validation and practical implementation of the seed-metering device.

5 Bench test validation

The bench testing platform was constructed using 4040 aluminum profiles and included the following major components: stepper motors (to independently drive the centrifugal disc and seed-metering wheel), the seed-metering device body, a DC power supply, motor drivers, a control system, seed collection units, and a data acquisition module. The test setup is illustrated in Fig. 14.

Bench tests repeated three times under the optimized parameters (involute guide strip, 49.01 r/min disc speed, 593.75 r/min wheel speed) yielded an average discharge rate of 2369 seeds/min, with a qualified seeding rate of 91.54% and a miss-seeding rate of 3.16%. The system met high-speed single-seed metering requirements with stable performance, low vibration and noise, and strong adaptability—demonstrating good potential for practical application.

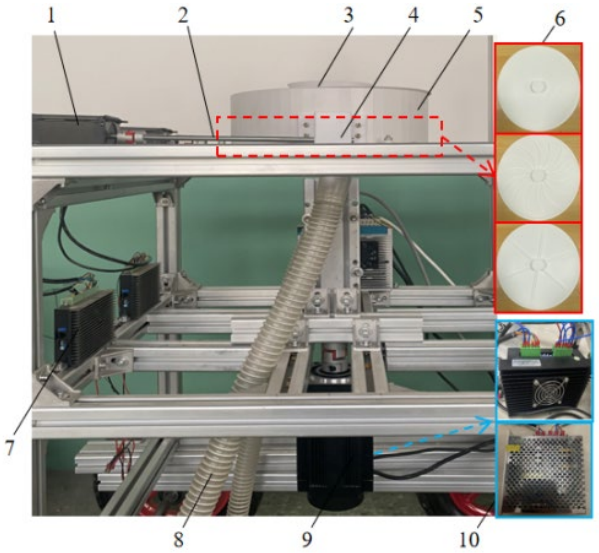

Figure 14. Test bench setup for performance validation. 1. Stepper motor 2. Slender shaft 3. Seed inlet 4. Seed dropping bag 5. Housing 6. Three types of seed discs 7. Actuator 8. Seed discharge pipe 9. Driving motor 10. Control system.
Source: Elaborated by the authors.

6 Conclusions

In response to the demand for high-speed, single-seed precision planting of soybean, a novel centrifugal seed-metering device was developed and systematically studied through simulation and experimental validation. The major conclusions are as follows:

Structural innovation:

A high-speed centrifugal precision seed-metering device was developed, featuring involute guide strips and ellipsoidal seed-holding grooves to ensure stable seed filling and orderly discharge under high-speed operation. In addition, the flexible metering wheel effectively reduced seed jamming and mechanical damage.

Simulation modeling and optimization:

A dynamic simulation model was developed in EDEM, and a second-order orthogonal rotational regression design was used to examine the effects of guide strip type, disc speed, and wheel speed on metering performance. Response surface analysis revealed nonlinear effects on both qualified and miss-seeding rates. The optimal combination—involute guide strip, 49.01 r/min disc speed, and 593.75 r/min wheel speed—yielded a qualified seeding rate of 92.08% and a miss-seeding rate of 1.91%.

Experimental validation and applicability:

Bench tests confirmed that, under optimized parameters, the device achieved a qualified seeding rate of 91.54% and a miss-seeding rate of 3.16%, consistent with simulation results and meeting national standards. The system demonstrated stable performance and good adaptability, supporting its application in high-speed precision planting.

References

[1] Tang, H, Xu F., Guan, T., Xu, Ch., and Wang, J., Design and test of a pneumatic type of high-speed maize precision seed metering device, Computers and Electronics in Agriculture, 211, art. 107997, 2023. DOI: https://doi.org/10.1016/j.compag.2023.107997

[2] Shang, S., Wu, X., and Yang, R., Research status and prospect of plot breeding seeding equipment and technology, Transactions of the Chinese Society for Agricultural Machinery, 52, pp.1-20, 2021. DOI: https://doi.org/10.6041/j.issn.1000-1298.2021.02.001

[3] Li, Y., Yang, L., and Zhang, D. Analysis and test of linear seeding process of maize high speed precision metering device with air suction, Transactions of the CSAE, 36(9), pp. 26-35, 2020. DOI: https://doi.org/10.11975/j.issn.1002-6819.2020.09.003

[4] Zhang, X., Cheng, J., Shi, Z., Zhang, Y., and Wang, M., Design and experiment of a clamp-holding precision maize- seed-metering device, Engenharia Agrícola, 42(6), art. 20220049, 2022. DOI: https://doi.org/10.1590/1809-4430-Eng.Agric.v42n6e20220049/2022

[5] Wang, W., Song, L., and Shi, W., Design and experiment of air-suction double-row staggered precision seed metering device for maize dense planting, Transactions of the Chinese Society for Agricultural Machinery, 55(3), pp. 53-63, 2024. DOI: https://doi.org/10.6041/j.issn.1000-1298.2024.03.005

[6] Zhang, M., Jiang, Y., and He, S., Design and experiment of the air suction wheel precision seed metering device for vegetables, Transactions of the CSAE, 39(7), pp. 98-109, 2023. DOI: https://doi.org/10.11975/j.issn.1002-6819.202211138

[7] Deng, Sh., Feng, Y., Cheng, X., Wang, X., Zhang, X., and Wei, Z., Disturbance analysis and seeding performance evaluation of a pneumatic-seed spoon interactive precision maize seed-metering device for plot planting, Biosystems Engineering, 247, pp. 221-240, 2024. DOI: https://doi.org/10.1016/j.biosystemseng.2024.09.007.

[8] Huang, Y., Li, P., and Dong, J., Design and experiment of side-mounted guided high speed precision seed metering device for soybean. Transactions of the Chinese Society for Agricultural

Machinery, 53(10), pp. 44-53+75, 2022. DOI: http://www.j-csam.org/jcsam/article/abstract/20221005?st=search

[9] Liu, W., Zhou, J., Zhang, T., Zhang, P., Yao, M., Li, J.; Sun, Z., Ma, G., Chen, X., and Hu, J., Key technologies in intelligent seeding machinery for cereals: recent advances and future perspectives, Agriculture, 15(1), art. 15010008, 2025. DOI: https://doi.org/10.3390/agriculture15010008

[10] Teixeira, S.S., dos Reis, A.V., and Machado, A.L.T., Longitudinal distribution of bean seeds in horizontal plate meter operating with one or two seed outlets, Engenharia Agricola, 33(3), pp. 569-574. 2013. DOI: https://doi.org/10.1590/S0100-69162013000300013

[11] Wang, Y., Li, H., and He, J. Parameter optimization and experiment of mechanical wheat shooting seeder, Transactions of the CSAE, 36(21), pp.1-10, 2020. DOI: https://www.aeeisp.com/nygcxb/en/article/Y2020/I21/1

[12] Liu, H., Guo, L., Fu, L., et al. Study on multi-size seed-metering device for vertical plate soybean precision planter, International Journal of Agricultural & Biological Engineering, [online]. 8(1), pp. 1-8, 2015. Available at: www.ijabe.net/article/doi/10.3965/j.ijabe.20150801.001

[13] Dun, G., Yang, Y., and Guo, Y., Analysis of EDEM simulation of different soybean seed filling characteristics, Journal of Henan Agricultural University, 53(01), pp. 93-98, 2019. DOI: https://doi.org/10.16445/j.cnki.1000-2340.2019.01.014

[14] Pan, X., Xia, X.., Gao, P., Ren, D., Hao, Y., Zheng, Z., Zhang, J., Zhu, R., Hu, B., Huang, Y., Double-setting seed-metering device for precision planting of soybean at high speeds, Transactions of the ASABE, 62(1), pp. 187-196, 2019. DOI: https://doi.org/10.13031/trans.13055.

[15] Shen, H., Zhang, J., Chen, X., Dong, J., Huang, Y., Shi, J., Development of a guiding-groove precision metering device for high-speed planting of soybean, Northwest A&F University, 64, pp. 1113-1122, 2021. DOI: https://link.cnki.net/doi/10.27409/d.cnki.gxbnu.2021.000943

[16] Zhang, R., Zhou, J., and Liu, H., Determination of interspecific contact parameters of corn and simulation calibration of discrete element, Transactions of the Chinese Society for Agricultural Machinery, 53(S1), pp. 69-77, 2022. DOI: https://doi.org/10.6041/j.issn.1000-1298.2022.S1.008

[17] Lei, X., Hu, H., Wu, W., Liu, H., and Liu, L., Seed motion characteristics and seeding performance of a centralized seed metering system for rapeseed investigated by DEM simulation and bench testing, Biosystems Engineering, 203, pp. 22-33, 2021. DOI: https://doi.org/10.1016/j.biosystemseng.2020.12.017

[18] Tang, Z., Xi, X., and Zhang, B., Design and test of an inter-row weeding machine applied in Soybean and Corn Strip Compound Planting (SCSCP), Agronomy, 14(9), pp. 2136-2136, 2024. DOI: https://doi.org/10.3390/agronomy14092136

[19] Chen, Y., Jia, H., and Wang, J., Design and experiment of scoop metering device for soybean high-speed and precision seeder, Transactions of the Chinese Society for Agricultural Machinery 48(8), pp, 95-104, 2017. DOI: https://dx.doi.org/10.6041/j.issn.1000-1298.2017.08.010

[20] Gao, X., Xie, G., Li, J., Shi, G., Lai, Q., and Huang, Y., Design and validation of a centrifugal variable-diameter pneumatic high-speed precision seed-metering device for maize, Biosystems Engineering, 227, pp. 161-181, 2023. DOI: https://doi.org/10.1016/j.biosystemseng.2023.02.004

[21] Ding, L., Yang, L., and Liu, S., Design of air suction high speed precision maize seed metering device with assistant seed filling plate, Transactions of the CSAE 34(22), pp. 1-11, 2018. DOI: https://www.tcsae.org/en/article/doi/10.11975/j.issn.1002-6819.2018.22.001

[22] Han, D., Zhang, D., and Jing, H., DEM-CFD coupling simulation and optimization of an inside -filling air-blowing maize precision seed-metering device, Computers and Electronics in Agriculture, 7(150), pp. 426-438, 2018. DOI: https://doi.org/10.1016/j.compag.2018.05.006

[23] Dun, G., Liu, W., and Mao, N., Optimization design and experiment of alternate post changing seed metering device for soybean plot breeding. Journal of Jilin University: Engineering and Technology Edition, pp. 53(1), 285-296, 2023. DOI: https://doi.org/10.13229/j.cnki.jdxbgxb20210570

Y. Zhang, is currently pursuing a Master's degree at the Institute of Modern Agricultural Equipment, Shandong University of Technology. His research direction is intelligent agricultural machinery and equipment engineering, and he has conducted in-depth research on high-speed precision seeding.
ORCID: 0009-0008-2376-3541

X. Zhang, obtained his Dr. degree from the China Agricultural University in 2016. He is currently a professor at the Institute of Modern Agricultural Equipment, Shandong University of Technology. His main research focuses on conservation tillage technologies and equipment, as well as the development of intelligent agricultural machinery and equipment. His research achievements have been recognized by peers at home and abroad.
ORCID: 0009-0003-9053-4398

X. Wang, obtained his Dr. degree from the China Agricultural University. He is currently a professor at the Institute of Modern Agricultural Equipment, Shandong University of Technology. His research interests include modern agricultural equipment and computer measurement and control.
ORCID: 0000-0001-7099-6286

X. Cheng, obtained his Dr. degree from the China Agricultural University. His research directions and fields include intelligent agricultural machinery and equipment.
ORCID: 0009-0001-0051-2968

Z. Wei, obtained his Dr. degree from China Agricultural University. His research areas include modern agricultural equipment and computer measurement and control.
ORCID: 0009-0005-4718-0074

P. Ma, is currently studying for a Master's degree at Shandong University of Technology, with his research focus on intelligent agricultural machinery and equipment engineering.
ORCID: 0009-0007-9380-1729